is not clear whether this activity is associated with mental aspects of tasks or with sensorimotor components, or with artifacts. In a previous study we found no topographic differences in EEG spectra between 15-second arithmetic, block rotation and letter substitution tasks after rigorously controlling other-than-cognitive factors (*2–4*). However, such heterogeneous tasks cannot be resolved into serial components reflecting different neurocognitive processes. We therefore refined our approach by using short (less than 1 second) tasks, using time references based on person-specific average ERP measurements, computing correlations between channels on a single-trial basis, and using mathematical pattern classification to reveal split-second sequential processing. This yielded a sequence of clear-cut between-task difference patterns involving split-second changes in the localization and lateralization of mass neural activity. Appropriate studies of neurocognitive functions should take into account this rapidly shifting network of localized and lateralized processes.

ALAN S. GEVINS
ROBERT E. SCHAFFER
JOSEPH C. DOYLE
BRIAN A. CUTILLO
ROBERT S. TANNEHILL
STEVEN L. BRESSLER

EEG Systems Laboratory,
1855 Folsom Street,
San Francisco, California 94103

References and Notes

1. E. Donchin, M. Kutas, G. McCarthy, in *Lateralization in the Nervous System*, S. Harnard *et al.*, Eds. (Academic Press, New York, 1977), pp. 339–384.
2. A. Gevins, G. Zeitlin, C. Yingling, J. Doyle, M. Dedon, R. Schaffer, J. Roumasset, C. Yeager, *Electroencephalog. Clin. Neurophysiol.* **47**, 693 (1979).
3. A. S. Gevins, G. M. Zeitlin, J. C. Doyle, C. D. Yingling, R. E. Schaffer, E. Callaway, C. L. Yeager, *Science* **203**, 665 (1979).
4. A. Gevins and R. Schaffer, *CRC Crit. Rev. Bioeng.* **1980**, 113 (1980).
5. A. S. Gevins, J. C. Doyle, R. E. Schaffer, E. Callaway, C. Yeager, *Science* **207**, 1006 (1980).
6. A. Gevins, in *Cerebral Hemisphere Asymmetry: Method, Theory and Application*, J. Hellige, Ed. (Praeger, New York, in press).
7. D. Friedman, R. Simpson, W. Ritter, I. Rapin, *Electroencephalog. Clin. Neurophysiol.* **38**, 13 (1975); C. Wood, *J. Exp. Psychol. Hum. Percep.* **104** (No. 1), 3 (1975); J. Marsh and W. Brown, *Prog. Clin. Neurophysiol.* **3**, 60 (1977); R. Thatcher, *Behav. Biol.* **19**, 1 (1977).
8. J. Hellige, Ed., *Cerebral Hemisphere Asymmetry: Method, Theory and Application* (Praeger, New York, in press).
9. M. Livanov, *Spatial Organization of Cerebral Processes* (Wiley, New York, 1977); J. Busk and G. Gailbraith, *Electroencephalog. Clin. Neurophysiol.* **38**, 415 (1975); E. Callaway and P. R. Harris, *Science* **183**, 873 (1974).
10. A. Gevins, *IEEE Trans. Patt. Anal. Machine Intell.* **2**, 383 (1980); S. Viglione, in *Adaptive Learning and Pattern Recognition Systems*, J. Mendel and K. Fu, Eds. (Academic Press, New York, 1970), pp. 115–163.
11. The two-layered, nonlinear, distribution-independent trainable classification-network algorithm used in this study is described in A. Gevins, J. Doyle, R. Schaffer, B. Cutillo, R. Tannehill, S. Bressler, *Electroencephalog. Clin. Neurophysiol.*, in preparation; and Gevins *et al.* (*12*).
12. A. Gevins, J. Doyle, G. Zeitlin, S. Bressler, *IEEE Trans. Patt. Anal. Machine Intell.*, in preparation.
13. A. S. Gevins, J. C. Doyle, B. A. Cutillo, R. E. Schaffer, R. S. Tannehill, J. H. Ghannam, V. A. Gilcrease, C. L. Yeager, *Science* **213**, 918 (1981). In the key for figure 3 of that report, $P < .005$ should have been next to the blank circle, while $P < .5 \times 10^{-5}$ should have been next to the hatched circle.
14. The stimulus subtended a visual angle of less than 2 degrees. The vertical position and side of screen of the target changed randomly across trials for both tasks, as did the horizontal angle and direction of the arrow. Response was made on a Grass isometric force transducer and varied randomly across trials from 0.1 to 1 kg. An individual trial consisted of a neutral warning that was followed after 2 seconds by the stimulus. One second after its completion the response was displayed.
15. Brain potentials were amplified with a Bioelectric Systems model AS-64P and Beckman Accutraces with a passband of about 0.1 to 50 Hz. Electroculogram and muscle potentials were amplified by a Grass model 6 with similar filter settings. All signals were digitized to 11 bits at 128 samples per second, and a 12-Hz, 15-point nonrecursive digital low-pass filter was applied.
16. A task-by-electrode-by-person analysis of variance of the P300 peak voltage revealed a significant task effect [$F(1, 8) = 29.0$, $P < .001$] and task-by-electrode interaction [$F(13, 104) = 2.9$, $P < .005$]. Correlated *t*-tests revealed P300 voltage enhancements in the no-move task for all but the lateral temporal electrodes; the most significant difference ($P < .0005$) was at the anterior midline parietal electrode. When corrected for multiple comparisons by the Bonferroni method only the right central, anterior, and posterior midline parietal electrodes reached significance ($P < .05$). P300 ERP peak amplitude increases have been associated with similar go versus no-go decisions [R. Simson, H. Vaughan, W. Ritter, *Electroencephalog. Clin. Neurophysiol* **43**, 864 (1977)] and with the perception of a novel or relevant stimulus. This study differs from typical P300 studies in that a difficult motor response is required to the more frequent stimulus.
17. A task-by-electrode-by-person analysis of variance of the slope of a straight line fitted to the slow-potential shift across the RP interval revealed a significant task effect [$F(1, 8) = 5.6$, $P < .05$], electrode effect [$F(14, 112) = 1.9$, $P < .05$], and task-by-electrode interaction [$F(14, 112) = 2.7$, $P < .005$]. Correlated *t*-tests showed larger move task slopes for nine electrodes; the most significant difference ($P < .005$) was at the left central electrode. When Bonferroni-corrected, no electrode reached significance at $P < .05$.
18. The N100–P200 and P300 centerpoints in milliseconds for each of the volunteers were: V1 (218, 452); V2 (200, 388); V3 (228, 482); V4 (210, 462); V5 (203, 398); V6 (208, 298); V7 (212, 368); V8 (181, 318); and V9 (203, 358). The RP interval was centered 135 msec after the P300 centerpoint.
19. The functions were derived from two-thirds of the data and were tested on the remaining one-third. This was repeated three times and the average test-set classification accuracy was computed. A test-set classification accuracy of 55 percent corresponds to $P < 5 \times 10^{-5}$. This is more than 3.8 standard deviations above the mean classification accuracy of 48 classifications using 1612 randomly labeled move and no-move trials. Mean accuracy on the randomly labeled data was 50.6 percent, with a standard deviation of 1.1 percent, an accuracy that could have occurred by chance with $P = .32$ according to the binomial distribution. High classification accuracy was not the objective. Rather, the relative classification accuracy of each electrode set was used as an indicator of anatomic and temporal localization of task-related patterns. The classification accuracy of the P300 and RP intervals assessed on each individual was at the chance level for only two of the nine people. Their data comprised only 9 percent of the total data set. When the entire analysis was performed on the data of one person (V7) in the P300 interval, the P4 electrode set again achieved the highest classification accuracy.
20. To select the most prominent correlations from significant classification functions, the pattern recognition analysis was applied recursively on the highest weighted correlations. Test-set classification accuracy based on the final three or four correlations was significant at $P < .001$ or better in each interval.
21. The P300 ERP peak has not been found to vary in lateralization specifically as a function of cognitive task (*1*). J. Desmedt [*Proc. Natl. Acad. Sci. U.S.A.* **74**, 4037 (1977)] reported a qualitative change in the ERP over the right hemisphere in a somatosensory-motor task, but the effect was general and was not present in the P300 peak.
22. We thank the late Gobind B. Lal for the "shadows of thought" metaphor; H. Currens for manuscript preparation and artwork; G. Gilcrease and J. Ghannam for assistance with recordings and analysis; R. Adey, M. Aminoff, P. Bach-y-Rita, F. Benson, E. Callaway, J. Engel, B. Garoutte, W. Gersch, R. Halliday, E. Roy John, B. Libet, J. Mazziotta, M. Mesulam, K. Pribram, J. Roumasset, A. Salamy, C. Skomer, J. Spire, H. Vaughan, D. O. Walter, C. Woods, and J. Vidal for valuable comments; J. Miller (Air Force School of Aerospace Medicine), D. Woodward (Office of Naval Research), A. Fregly (Air Force Office of Scientific Research), J. Fetzer, and M. Bachman-Hoffman for research support.

19 November 1982; revised 1 February 1983

A Functional Role for an Opiate System in Snail Thermal Behavior

Abstract. *The terrestrial snail* Cepaea nemoralis, *when placed on a 40°C hot plate, lifts the anterior portion of its foot. The latency of this response is influenced by morphine and by naloxone in a dose-dependent and time-dependent manner. Morphine increases the time taken to respond, whereas naloxone reduces it. Furthermore, naloxone abolishes the effect of morphine. These results indicate that an opiate system may have a role in this behavior, which resembles that reported in vertebrates.*

Although the importance of opiate systems in mediating behavioral and physiological activities is recognized in vertebrates (*1*), the role of opiate systems in invertebrates has only recently become apparent (*2–4*). Evidence for electrophysiological and biochemical effects of opiates, their agonists, and antagonists and the demonstration of specific opiate receptors in molluscs (*3*), have resulted in the suggestion that opiate receptors and their effectors play a role in the regulation of transmitter release in invertebrates (*4*). We present evidence that opiate systems have a functional role in determining the thermal behaviors of the terrestrial snail *Cepaea nemoralis*.

The snails were maintained as sepa-

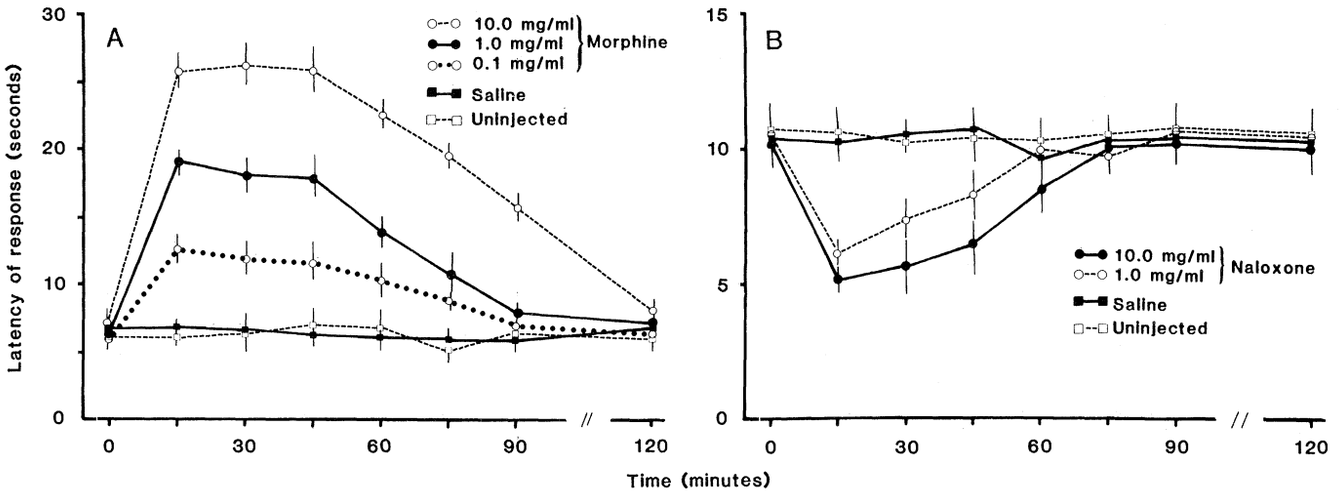

Fig. 1. Time courses of the effects of (A) morphine (1.0 μl at 0.1, 1.0, and 10.0 mg/ml) and (B) naloxone (1.0 μl at 1.0 and 10.0 mg/ml) on the latency of the foot-lifting response to heat in two different morphs of *C. nemoralis*. Controls were given saline injections (1.0 μl) or no injections. Ten different individuals were used for each dose and treatment. Vertical lines denote two standard errors. Note the change in scale between A and B.

rate morphs (*5*) under natural conditions of photoperiod and temperature (14 hours of light and 10 hours of darkness at 22° to 30°C), with food and water freely available (*6*). Thermal detection and avoidance behaviors of the snails were evaluated with our modification of a technique used by Woolfe and Macdonald (*7*). Individual snails were placed on a hot plate (*8*) at 40° ± 0.5°C, and the latency of their foot-lifting response (5 to 10 seconds) to the thermal stimulus was recorded. A stereotypical elevation of the anterior portion of the extended foot was observed in fully hydrated snails (*9*) that were exposed to a heat stress. This foot-lifting behavior was never observed in snails exposed to ambient or nonstressful thermal conditions (*10*).

The effects of morphine sulfate (1 μl at concentrations of 0.10, 1.0, or 10.0 mg/ml) and naloxone hydrochloride (1 μl at 1.0 or 10.0 mg/ml) on the latency of the thermal responses of single *C. nemoralis* were determined. Single morphs were used in order to reduce variabilities in the responses (*5*). The opiate agonist or antagonist (1 μl) was injected with a 10-μl Hamilton syringe into the side of the foot either in the vicinity of the mantle cavity or directly into it. Individuals receiving saline vehicle (*11*) injections or no injections were used as controls. All determinations were carried out in the early photophase (900 to 1100 hours at 25° to 27°C ambient temperature) with only one treatment per individual. Each treatment was replicated ten times for each morph. No corrections in dosage were made for variations in the mass of the individual snails (*12*).

Administration of morphine resulted in a significant ($P < .001$, *t*-test; at 1.0 mg/ml) dose-dependent increase in the latency of the foot-lifting response (Fig. 1A). The maximum effects of morphine occurred 15 to 45 minutes after injection and the effects of morphine disappeared in 90 to 120 minutes. Saline treatment had no detectable effects on the latency of the foot-lifting response (Fig. 1A). The increased variability in responses obtained with the highest (10 mg/ml) dose of morphine may be in part attributed to disruptions of locomotor behavior as some of the snails became more sluggish in their movements. The dose-dependent and time-dependent behavioral effects of morphine are analogous to the effects reported in mammals given opiates (*13*). However, *C. nemoralis* are probably more sensitive to opiate-induced antinociception than mammals are (*13*). Administration of naloxone (1 μl at 1 mg/ml) along with morphine (1 μl at 10 mg/ml) blocked the increase in latency, indicating effects at specific opiate receptors. Administration of naloxone by itself resulted in a significant ($P < .01$, *t*-test; for 1 μl at 1.0 mg/ml) decrease in the latency of response to the thermal stimulus, with maximum effects evident 15 minutes after treatment (Fig. 1B). This effect of naloxone supports the hypothesis of a direct role for endogenous opiate systems in snail thermal behavior; further investigations of possible nonspecific effects are needed (*14*). In general, naloxone does not have consistent significant effects on vertebrate behavioral responses to many aversive stimuli (*15*).

Our results suggest that opiate systems have a functional role in snail thermal behaviors and imply that this role is in many respects comparable to that reported for mammalian behaviors. Therefore, molluscs, and in particular snails, might serve as useful, sensitive models for evaluating the behavioral effects of biologically active vertebrate peptides and their synthetic analogs. This is of particular significance in view of the recent evidence for a neuroregulatory role in mammals of a molecule similar or possibly identical to the molluscan opiate-like peptide FMRFamide (*16*). The opiate effects in *C. nemoralis* may arise either through direction alterations in neuronal activity or more likely through modulation of neurotransmitters, in particular that of the dopamine-mediated system (*2*).

MARTIN KAVALIERS
MAURICE HIRST
G. CAMPBELL TESKEY
Department of Zoology and Department of Pharmacology and Toxicology, University of Western Ontario, London, Ontario N6A 5B7, Canada

References and Notes

1. G. C. Davis, M. S. Buchsbaum, W. E. Bunney, *Ann. N.Y. Acad. Sci.* **362**, 67 (1981); H. Imura and Y. Nakai, *Annu. Rev. Physiol.* **43**, 265 (1981); A. Pert, *Adv. Neurol.* **33**, 107 (1982).
2. G. B. Stefano, I. Vadaz, L. Hiripi, *Experientia* **36**, 667 (1980); G. B. Stefano, K. S. Rosza, L. Hiripi, *Comp. Biochem. Physiol.* C **66**, 193 (1980); H. Maldonado and A. Miralto, *J. Comp. Physiol.* **147**, 455 (1982); K. Lukowiak, J. A. Thornhill, J. Edstrom, *Regul. Peptides* **3**, 303 (1982); G. B. Stefano and E. J. Catapane, *Life Sci.* **24**, 1617 (1979); G. B. Stefano and L. Hiripi, *ibid.* **25**, 291 (1979); N. N. Osborne and V. Neuhoff, *J. Pharm. Pharmacol.* **31**, 481 (1979); G. B. Stefano, B. Hall, M. H. Makman, B. Dvorkin, *Science* **213**, 928 (1981).
3. G. B. Stefano, R. M. Kream, R. S. Zukin, *Brain Res.* **181**, 440 (1980); R. M. Kream, R. S. Zukin, G. B. Stefano, *J. Biol. Chem.* **255**, 9344 (1980).
4. B. Costall, D. H. Fortune, R. J. Maylor, *Eur. J. Pharmacol.* **49**, 46 (1978); M. F. Chesselet, A. Chermay, T. D. Reisine, J. Glowinski, *Nature (London)* **291**, 320 (1981); S. Konishi, A. Tsunoo, M. Otsuka, *ibid.* **294**, 80 (1981).
5. *Cepaea nemoralis* is genetically and to a lesser extent behaviorally polymorphic [J. S. Jones *et al.*, *Annu. Rev. Ecol. Syst.* **8**, 109 (1977)]. This is visually evident in morphs of different shell colors, pink or yellow, coupled with banding patterns. Preliminary investigations revealed variations in response between morphs.

6. Snails were fed daily with lettuce supplemented with vitamins. Water was freely available at all times.
7. G. Woolfe and A. D. Macdonald, *J. Pharmacol. Exp. Ther.* **80**, 300 (1944).
8. The hot plate was made by Technilab Instruments, Inc., Dequannock, N.J.
9. Terrestrial snail activity has been shown to be affected by hydration state [L. H. Smith, Jr., *Physiol. Zool.* **54**, 407 (1981)]. In our study, all snails tested were allowed to hydrate fully in sealed containers with a saturated atmosphere and water in the bottom. Hydrated individuals had a fully extended foot and were actively moving in the container.
10. Control experiments were conducted with the hot plate at lower temperatures (20° to 35°C). In addition, snail activity was monitored in thermal gradients and in field situations (B. Goodson, in preparation). Under normal thermal conditions this foot-lifting behavior was absent. *Cepaea* can display a "rearing" behavior in response to tactile stimulation of the head tentacles. This rearing involves an elevation of the entire body, including the shell, and is similar to the behaviors described for *Helix* [R. A. Everett, R. S. Ostfeld, W. J. Davis, *Z. Tierpsychol.* **59**, 109 (1982)].
11. Physiological saline consisted of NaCl, 80 m*M*; KCl, 5 m*M*; $CaCl_2$, 7 m*M*; $MgCl_2$, 5 m*M*; and tris buffer, 5 m*M*; final *p*H 7.8 [K. Meng, *Naturwissenschaften* **19**, 470 (1958)].
12. The snail body mass without a shell was 0.70 to 1.30 g.
13. R. W. Smith, M. Hirst, C. W. Gowdey, *Arch. Int. Pharmacodyn. Ther.* **221**, 266 (1976).
14. J. C. Sawynok, J. C. Pinsky, F. S. LaBella, *Life Sci.* **25**, 1621 (1979).
15. F. C. Tulmay, S. B. Sparker, A. G. Takenou, *Eur. J. Pharmacol.* **33**, 65 (1975); A. Goldstein, G. T. Pryor, L. S. Otis, F. Larsen, *Life Sci.* **18**, 599 (1976); A. Pert and M. Walter, *ibid.* **19**, 1023 (1976); R. J. Bodnar, D. D. Kelly, A. Spiaggig, C. Ehrenberg, M. Glusman, *Pharmacol. Biochem. Behav.* **8**, 667 (1978).
16. G. J. Dockray, C. Valliant, R. G. Williams, R. J. Gayton, N. N. Osborne, *Peptides* **2** (Suppl.) 25 (1981); R. J. Gayton, *Nature (London)* **298**, 275 (1982).
17. We thank B. Goodson for care of the snails, I. Craig for photographic skills, and Endo Laboratories, Inc., for a generous supply of naloxone hydrochloride. Supported by Natural Sciences and Engineering Research Council of Canada grant S222A1 (to M.K.) and Medical Research Council grant MA-7278 (to M.H.).

13 August 1982; revised 21 December 1982

Mechanical Measurement of Red Cell Membrane Thickness

Abstract. *The thickness of intact human red cell membrane is measured by a light-microscope technique in which membrane material with a known surface area is extracted into a long, thin cylindrical strand. The radius of the strand is calculated from its known length and surface area. The minimum radius, obtained at high extraction velocities or large membrane tensions, is 55 angstroms. A collapsed membrane cylinder with a mean-mass radius of 55 angstroms would have a membrane thickness of 78 angstroms.*

Benjamin Franklin observed (*1*) that one teaspoon of oil (4.93 cm^3), when allowed to spread on Clapham pond, would cover about ½ acre (2.02×10^7 cm^2). If we assume that the volume of oil in Franklin's experiment remains constant during the spreading process, then we can easily calculate that the thickness of the oil film is 24 Å. Thus, a submicroscopic dimension is readily calculated from macroscopic measurements such as, in this case, surface area and volume. In this spirit, we have devised an experimental technique that permits calculation of red cell membrane thickness, using only the "principle of conservation of membrane surface area" and measurements made with a light microscope.

In our experiments we allow nearly spherical fresh human red cells suspended in a hypotonic phosphate-buffered solution (*p*H 7.4, 160 mos*M*, 0.05 to 0.08 g percent albumin) to settle and adhere to latex beads 2 μm in diameter, forming cell-bead pairs. Subsequently, we aspirate a portion of the cell membrane into a small glass pipette and capture the latex bead with another smaller glass pipette, thereby suspending the cell and bead between two pipettes (Fig. 1A). Movement of the bead and smaller pipette away from the cell results in the formation of a long, thin membrane filament or "tether" (*2*), observed as a faint shadow stretched between the cell body and the point of membrane attachment (Fig. 1, C and D). As we increase the aspiration pressure and thus the isotropic tension in the membrane (*3*), the cell becomes more spherical, and the tether shadow becomes fainter as the tether diameter decreases until it disappears from view (Fig. 1A). Reducing the tension results in elongation of the cell and reappearance of the tether. In Fig. 1B a schematic of the aspirated cell and formed tether shows a greatly magnified end-on view of the tether indicating the phospholipid bilayer membrane geometry.

Initially, it would seem impossible to measure in situ something as thin as a tether. However, the method of tether formation shown in Fig. 1 permits us to measure the tether radius as it is formed. In essence, a reservoir of membrane material is sucked into the pipette. As we pull the tether from the cell body, the membrane material in the pipette is reduced. Since the aspiration pressure is held constant during tether formation (or reabsorption), this process occurs at constant membrane surface area and constant cell volume (*4*). For the sake of illustration, we write that the decrease in membrane material within the pipette is balanced by an increase in membrane material in the tether:

$$-2\pi R_p dL_p \approx 2\pi R_t dL_t \qquad (1)$$

where R_p is the (measurable) radius of the pipette, $-dL_p$ is the (measurable) decrease in length of the aspirated por-

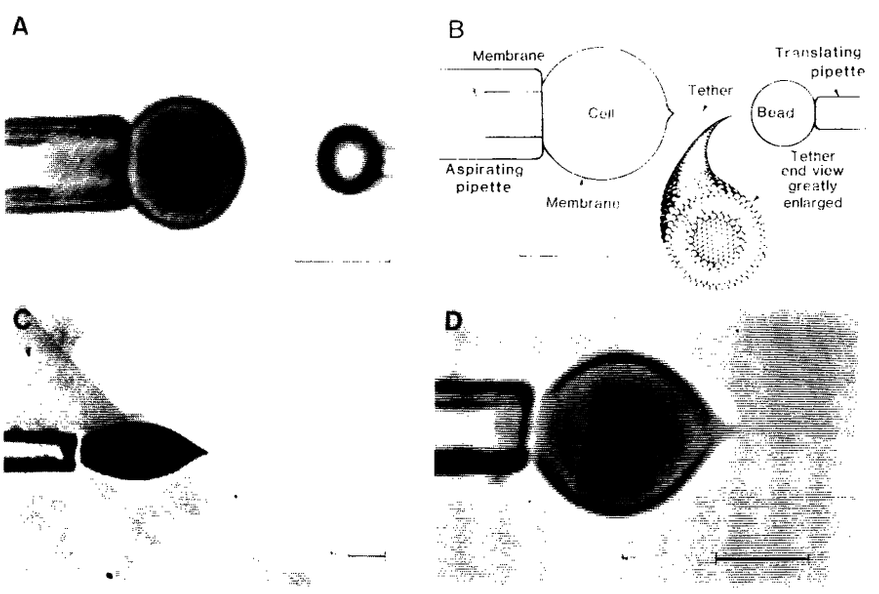

Fig. 1. Photographs taken from a video monitor of tethered red cells. (A) Red cell aspirated into the larger pipette and latex bead held by the smaller pipette. The (invisible) tether is stretched between cell and bead. (B) Schematic of (A) showing a greatly magnified end-on view indicating the phospholipid bilayer membrane geometry. (C) Flaccid red cell with a relatively thick tether. (D) Partially sphered cell. Note how the tether pulls on the cell body. An increase in the aspiration pressure causes the cell to assume a nearly spherical shape (A) and aspirates more membrane material into the pipette. However, the tether still produces a small amount of cell distortion at a "point" on the cell membrane opposite the point of aspiration. Scale bars, 4 μm.